Electron impact excitation of the Hg($6^3P_{0,2}$) metastable states*

H. F. Krause, S. G. Johnson,† and S. Datz
Chemistry Division, Oak Ridge National Laboratory, Oak Ridge, Tennessee 37830
(Received 23 July 1976)

Electron impact excitation functions for the Hg($6^3P_{0,2}$) metastable states were measured from threshold to 8.5 eV. The $6^3P_{0,2}$ states were detected by monitoring the forbidden photon emission. The 6^3P_2 state was also selectively detected by monitoring the 2537-Å emission from collisional deexcitation to the 6^3P_1 state followed by radiative decay to 6^1S_0. Structure observed in the excitation functions appears to be due to autoionization of short-lived excited states of Hg^-. The ratio of cross sections for formation of the $6^3P_{2,0}$ states, σ_2/σ_0, determined at the peak of the 6^3P_2 excitation function ($E \simeq 5.8$ eV), is 9.1. The ratio of cross sections at the peak of each excitation function (6^3P_2, $E \simeq 5.8$ eV; 6^3P_0, $E \simeq 5.2$ eV) is 5.2.

I. INTRODUCTION

In the course of crossed-molecular-beam studies of chemiluminescent reactions involving metastable Hg($6^3P_{0,2}$) atoms and halogenated molecules,[1] accurate knowledge of relative beam populations of the metastable atoms produced by electron impact excitation was required. Survey of the literature indicated that excitation functions for the $6^3P_{2,0}$ states[2-4] has been measured recently using different detection methods: (1) Auger electron ejection, and (2) electrons superelastically scattered from Hg*. The 6^3P_2 excitation function of Borst[2] (method 1) disagreed considerably with that of Korotkov and Prilezhaeva[3] (method 2). The 6^3P_0 excitation function had been measured only by Korotkov[4] (method 2). The work of Korotkov for the $^3P_{2,0}$ states would have satisfied our needs had it not been for the fact that we had already measured the $^3P_2$ excitation function using a third method (described in this paper) and had found close agreement only with Borst. Therefore, it became necessary for us to measure independently the $^3P_0$ excitation function and the ratio of the $^3P_2$ and $^3P_0$ excitation cross sections, σ_2/σ_0.

Our initial attempt employed selective detection of the $6^3P_{0,2}$ states by optical excitation fluorescence involving the $6^3P_{0,2} \rightleftharpoons 7^3S_1$ transitions. The preliminary experiments led to unacceptably large error limits on both the $^3P_0$ excitation function and on σ_2/σ_0.[5] Although all difficulties encountered could have been corrected readily, this extremely sensitive and selective method of detection was abandoned in favor of direct optical detection of the Hg($6^3P_{0,2}$) forbidden-line emission.

Detection of long-lived metastable species ($\tau > 1$ sec) produced by electron impact by monitoring the forbidden-line radiation is often assumed to be impractical. In this work, we have demonstrated feasiblility of the method in an experimental arrangement designed specifically for cross-beam collisional studies using only electron energy spreads adequate for our purposes ($\Delta E \simeq 0.25$ eV FWHM).

Since this beam arrangement did not maximize the collection solid angle or the emitting volume, we estimate that increased signal yields of order 10–100 could have been achieved easily by specific design. These improvements alone, coupled with state-of-the-art detectors, indicate that forbidden-line monoenergetic-electron-impact studies are now feasible for metastable species having an excitation-cross-section to lifetime ratio, σ/τ, greater than or equal to that of Hg(6^3P_0) ($\simeq 10^{-17}$ cm^2/sec).

II. PRINCIPLES OF THE EXPERIMENT

The 6^3P_2 and 6^3P_0 metastable states of Hg lie 5.460 and 4.667 eV[6] above the 6^1S_0 ground state, and these states give rise to the 2269.8- and 2655.6-Å forbidden lines when they radiatively decay to the ground state. Many years ago, Mrozowski[7,8] observed directly the hyperfine structure of these lines and showed that the emission was due only to the two odd mercury isotopes 199 and 201 with nuclear spins $\frac{1}{2}$ and $\frac{3}{2}$. Since the even isotopes of Hg have no nuclear spin, this observation is consistent with the angular momentum selection rule for electric dipole transitions when hyperfine structure is considered ($\Delta F = 0, \pm 1; 0 \not\rightarrow 0; F = J + I$). Subsequently, Garstang[9] performed refined calculations of the electric dipole transition probabilities for both of these forbidden lines which indicate lifetimes for the $6^3P_{0,2}$ states of 5.56 and 6.67 sec, respectively (for the terrestrial isotopic ratio), assuming this is the principal mode of decay. Garstang[10] also calculated the magnetic quadrupole transition probability for $6^3P_2 \rightarrow 6^1S_0$, and found it to be a factor of 42 smaller than for electric dipole transitions. The $6^3P_0 \rightarrow 6^1S_0$ transition is

strictly forbidden via the magnetic quadrupole decay mode.

The experimental arrangement employed to study the forbidden-line emission is shown in Fig. 1. Mercury atoms in the ground state issued from a thermal source through a multicapillary array, and this beam passed through a current-regulated electron beam. The electron beam was confined spatially by a static magnetic field, and its energy was reasonably well defined at the electron current densities employed. The excited atom beam formed at this point traveled a short distance to the region where spontaneous beam emission was detected in a direction perpendicular to the electron beam direction. The detector consisted of collection and focusing lenses, a grating monochromator, and a cooled photomultiplier tube.

Since it is well known that radiation from atoms excited by electron impact is usually partially polarized (electron energy dependent), we took steps to minimize some possible effects on the results. First, any polarization of excited atoms at the point of excitation would have been reduced during flight to the detection region due to collisional depolarization. For example, considering the self-depolarization cross section for $Hg(6\,^3P_2)$ along,[11,12] and the experimental geometry and conditions given below, any original polarization had to be reduced by at least the factor ≤ 0.7 (see Sec. III). Secondly, a plane polarizer was introduced at the monochromator entrance slit which was used to adjust the total detector polarization factor $\epsilon^{\parallel}(\lambda)/\epsilon^{\perp}(\lambda)$ to be $\frac{1}{2}$ (where $\parallel$ and $\perp$ on the detection efficiency factors ϵ refer to the electron beam direction) at each forbidden wavelength λ employed in these studies. Woolsey and McConkey have shown[13] that this instrumental polarization eliminates the need for polarization corrections to emission intensity when electric dipole radiation is viewed at 90° to the electron beam direction. Of course, this does not constitute perfect elimination of polarization effects in our arrangement because of the moderately large detection solid angle.

When the spontaneous beam emission at 2270 or 2656 Å due to the $6\,^3P_2$ or $6\,^3P_0$ state was examined, count rates were very low (~ 0.1 counts/sec) when narrow monochromator slits were used in order to accurately verify the emission wavelengths ($\Delta\lambda = 1.5$ Å). Much higher count rates (~ 1.0 counts/sec) required for excitation function measurements were achieved by the use of wide monochromator slits and the introduction of a mercury absorption cell before the monochromator (see Fig. 1). A heated absorption cell ($\simeq 80\,^{\circ}C$; path length 2 cm) was required in order to eliminate intense 2537-Å emission that could interfere with the forbidden-line beam emission at 2656 Å. The 2537-Å emission was due principally to reaction (1): intramultiplet relaxation of $Hg(6\,^3P_2)$ atoms by molecular constituents of the residual gas[14]:

$$\begin{aligned} Hg(6\,^3P_2) + N_2 &\rightarrow Hg(6\,^3P_1) + N_2^{\ddagger} \\ &\searrow Hg(6\,^1S_0) + h\nu\,, \end{aligned} \tag{1}$$

where $N_2^{\ddagger}$ indicates vibronic excitation. The cell was evacuated and outgassed before the mercury was introduced and then sealed in order to eliminate the possibility of 2656-Å forbidden-line production within the cell produced by 2537-Å light being absorbed and re-radiated by intramultiplet conversion scheme (2):

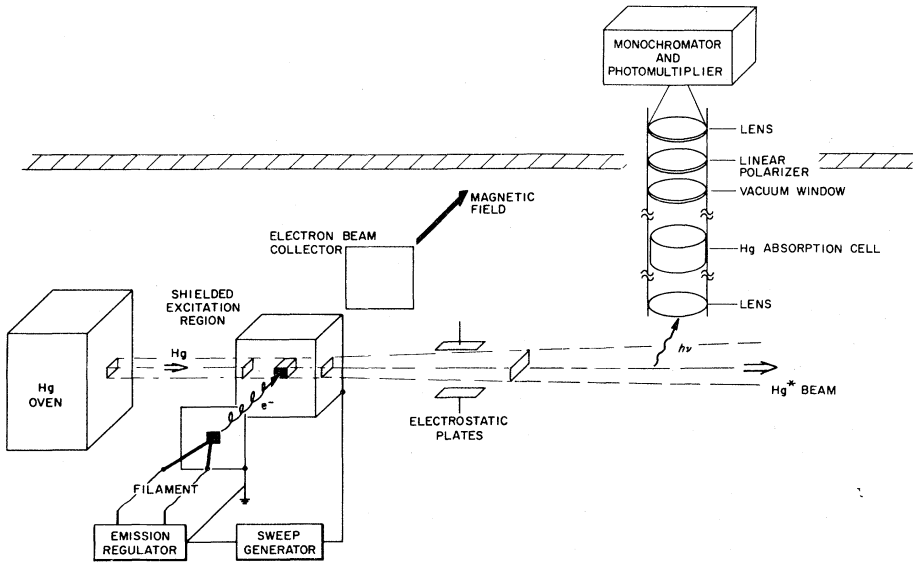

FIG. 1. Sketch of the experimental arrangement. Liquid-nitrogen-cooled trapping and collimation associated with the Hg beam is not shown.

$$h\nu(2537\ \text{Å}) + \text{Hg}(6\,^1S_0) \rightarrow \text{Hg}(6\,^3P_1)$$
$$\text{Hg}(6\,^3P_1) + M \rightarrow \text{Hg}(6\,^3P_0) + M^{\ddagger}$$
$$\searrow \text{Hg}(6\,^1S_0) + h\nu(2656\ \text{Å}). \qquad (2)$$

The resolution employed when measuring the $^3P_0$ excitation function was $\simeq 120$ Å which excluded the $^3P_2 \rightarrow {}^1S_0$ forbidden line.

The Hg($6\,^3P_2$) excitation function was also measured via quenching reaction (1) (here the absorption cell was cooled to liquid-nitrogen temperature to remove the Hg vapor). The 2537-Å emission was enhanced (200:1) by admission of a nitrogen beam which intersected the excited mercury beam in the viewing region. The 2537-Å radiation intensity was then measured as a function of bombarding electron energy. The contribution of 2537-Å light from Hg($^3P_0$) in the beam via (3) was negligible since its rate is less than 10^{-3}, that of reaction (1)[15] due principally to reaction endoergicity (0.2 eV):

$$\text{Hg}(6\,^3P_0) + \text{N}_2 \rightarrow \text{Hg}(6\,^3P_1) + \text{N}_2$$
$$\searrow \text{Hg}(6\,^1S_0) + h\nu. \qquad (3)$$

The availability of radiative transition probabilities for the Hg($6\,^3P_{0,2}$) states greatly simplifies measurement of relative electron impact excitation cross sections. The forbidden-line intensities $I(\lambda)$ corrected for detection efficiency factors are related to the electron-energy-dependent excitation cross sections $\sigma_i(E)$ for the $i = 0, 2$ metastable states ($^3P_0$, $^3P_2$, respectively) in Eq. (4):

$$\frac{I(2270\ \text{Å})}{I(2656\ \text{Å})} = \frac{\sigma_2(E)}{\sigma_0(E)} \frac{A_2}{A_0}. \qquad (4)$$

The A_i are radiative transition probabilities averaged over the natural Hg isotopic mixture. Other factors, such as ground-state mercury-atom density, effective volume detected, and electron current density are experimental constants, and therefore cancel in Eq. (4). Survival factors that express the relative collisional loss for each of the metastable states produced in traveling between the production and observation points, are excluded from Eq. (4) because the maximum integrated attenuation for either beam must have been less than 3% based on known $6\,^3P_{0,2}$ collisional deactivation cross sections[14-17] for Hg and atmospheric constituents of the 10^{-6}-Torr vacuum. This upper limit estimate is essentially due to the state-changing, self-collisional deactivation processes (Hg* + Hg) of the type Hg($^3P_2 \rightarrow {}^3P_{0,1}$), Hg($^3P_{0,2} \rightarrow {}^1S_0$) ($\sum \sigma_d \simeq 50$ Å^2, $n_{\text{Hg}} \lesssim 3 \times 10^{12}$ atoms/cm^3) because the state-changing intermolecular processes involving residual atmospheric gases (e.g., Hg* + N_2, O_2, H_2O, etc.) have smaller summed cross sections[14-17] and the abundance of the molecular constituents is very much smaller in the 10^{-6}-Torr vacuum. Also, the integrated beam attenuation via radiative decay is much smaller than that due to collisional loss.

III. APPARATUS

The excited-atom source employed in these studies differed from that previously described,[14] and it is sketched in Fig. 1. Electrons from a heated length (hairpin shaped) of thoriated iridium ribbon (20×2 mm) were accelerated to the anode ($\simeq 0.5$ mm away) through a potential of typically 20 V. The total emission current (temperature limited) was regulated according to principles previously discussed.[18] About 0.5% of the anode current passed into the excitation region where it was decelerated to its final energy. The electron current which intersected the atomic beam ($n_{\text{Hg}} \simeq 3 \times 10^{12}$ atoms/cm^3, 4.0 mm from array) was collected outside this carefully screened region at a potential of 50 V. The excitation region was kept small (length of sides 8 mm) in an attempt to decrease the space-charge depression. The source was immersed in a static magnetic field (~ 80 G), and the residual field in the optical observation region (~ 5 G) was essentially parallel to that at the point of excitation and at all points in between.

The possibility exists that reflected electrons (i.e., electrons reflected from the collector surface which are constrained by the magnetic field to motion back through the excitation region) could affect the excitation function measurements. The reflection coefficient is a function of the collector surface and incident electron energy. Our collector surface was stainless steel probably coated with Hg, and its reflection coefficient was not measured; however, the electron energy at the collector was held fixed at 70 eV throughout the electron-energy sweep range. Thus, the reflected electron fraction was constant as a function of electron bombardment energy in the screened region (see Fig. 1) and would not affect the shape of the separate excitation functions. Moreover, the relative $^3P_2/^3P_0$ cross sections would be similarly unaffected.

The two-chambered mercury oven was also temperature regulated. The metastable beam was previously shown to have a long-term stability of $\pm 2\%$ for the $^3P_2$ state ($E \simeq 5.8$ eV) for continuous operation periods of 200 h after an initial 24-h stabilization period. The metastable beam was exposed to a transverse electric field (~ 18 V/cm) before reaching the observation region in the unlikely event of a long-lived (Hg$^-$)* beam component.

The center of the observation region was located 3 cm from the point of excitation, and the light emitted was collected by an $f/1$ fused-silica lens located a focal length away. The collected light passed out of the vacuum through a fused-silica window and a linear polarizer (Polacoat) and was refocused ($f/4$) onto the grating monochromator entrance slit (Jarrel-Ash, $\frac{1}{4}$ m, 3000-Å Blaze). Light from the grating was imaged onto a small spot of the 9558 QB photomultiplier by a fused-silica lens system. Photomultiplier dark count (~1.9 counts/sec) was achieved by magnetic focusing at the photo cathode and by cooling the tube to $-20\,^{\circ}$C.

Excitation functions were accumulated on a multiscaling system by linearly sweeping the electron beam energy through the excitation potential region of interest. The average potential of each accumulation was simultaneously digitized via voltage-to-frequency converters on both the emission regulator and the sweep generator, and automatically recorded. The electron beam current was also digitized and integrated over each observation time.

IV. RESULTS

A. Hg($6\,^3P_{0,2}$) excitation functions

The excitation functions measured for $6\,^3P_2$ (voltage sweep rate 0.05 V/20 sec) and $6\,^3P_0$ (0.1 V/600 sec) via intramultiplet relaxation and spontaneous emission, respectively, are shown in Fig. 2. For each, the electron current was 0.7×10^{-6} A (±3% throughout scanning range) for an estimated current density of 15×10^{-6} A/cm^2. A constant background was subtracted from the sum of 5 consecutive scans, and the error limits shown are ±2 standard deviations.

The electron energy calibration was performed in the following manner. Noticing that the measured $^3P_2$ excitation function agreed most closely with that obtained by Borst[2] (see Fig. 3), our electron-energy scale was adjusted for best fit between the experiments in the 5.7-eV region. This was reasonable because his electron-energy resolution (RPD technique) was superior to ours. If we had established our scale by linear extrapolation of the data to threshold, the scale would have been displaced about 0.15 V above that shown in Fig. 2. As a consequence, we estimate an electron-energy resolution of order 0.25 eV (FWHM). $6\,^3P_2$ excitation functions were also measured at increased electron current densities, and the data did not begin to show noticeable shift to higher applied potential until the electron current was increased beyond a factor of 3. From this we conclude that the space-charge depression at the excitation point was less than $\simeq 0.1$ eV for the original data and that our energy scale was linear throughout the sweep range shown.

B. Excitation cross-section ration, σ_2/σ_0

The excitation cross-section ratio σ_2/σ_0 at $E=5.75$ eV ($\Delta E\simeq 0.25$ eV) was deduced from spontaneous emission intensities, as discussed in Sec. II.

The experimental procedure was as follows. First, the instrumental polarization (polarizer shown in Fig. 1 included) was set to be $\epsilon^{\parallel}\,\epsilon_{\perp}(\lambda)=\frac{1}{2}$ for λ either 2270 or 2656 Å by rotating the linear polarizer with polarized light incident on the configuration at approximately these wavelengths. The light source was NO ($A\,^2\Sigma^+\rightarrow X\,^2\Pi$) radiation centered at either 2265 Å ($v'=0\rightarrow v''=0$ band) or

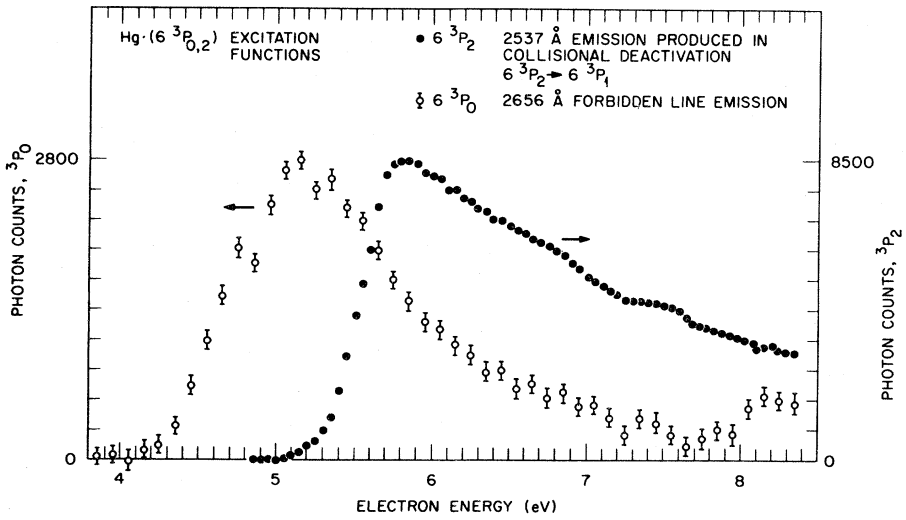

FIG. 2. Excitation functions for the $6^3P_{0,2}$ states. Photon counts in the peak of each excitation function have been normalized. The electron-energy calibration was set by comparing the $^3P_2$ excitation function with that of Borst (see Fig. 3 and text). The energy scale of the $^3P_0$ measurement relative to that of $^3P_2$ is estimated to be ±0.10 eV.

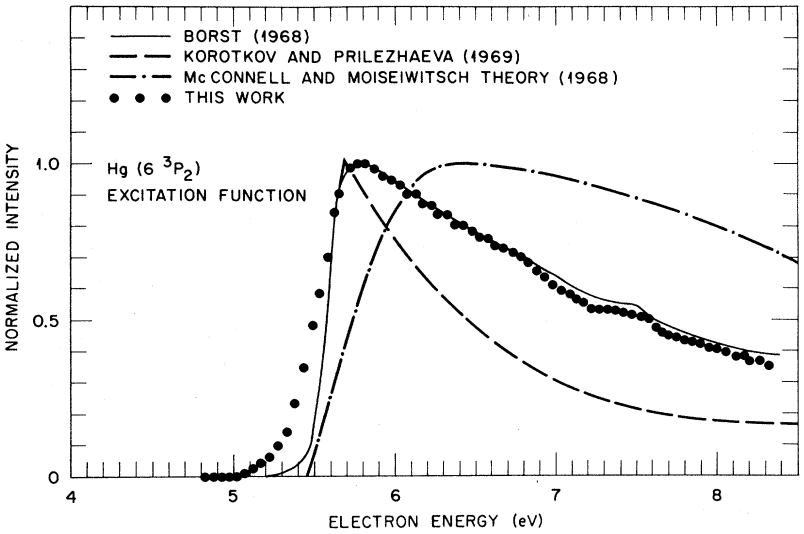

FIG. 3. Experimental and theoretical excitation functions for Hg($6\ ^3P_2$). The excitation functions have been normalized to the same peak value. Data of Fig. 2 are shown.

2717 Å ($v' = 0 \rightarrow v'' = 4$ band) produced in the near-resonant crossed-beam excitation transfer reaction,[19]

$$\mathrm{Hg}(6\,^3P_2) + \mathrm{NO}(X\,^2\Pi) \rightarrow \mathrm{NO}(A\,^2\Sigma^+, v' = 0) + \mathrm{Hg}(6\,^1S_0)$$
$$\searrow \mathrm{NO}(X\,^2\Pi) + h\nu . \qquad (5)$$

The emission was assumed to be initially unpolarized, and it was polarized parallel and perpendicular to the electron beam direction using a second linear polarizer. Since the 2656-Å forbidden line lies about midway between the $0 \rightarrow 3$ (2590 Å) and $0 \rightarrow 4$ bands of NO($A \rightarrow X$), the setup polarization was checked at 2590 Å and found to agree with that setup at 2717 Å within 10%.

Second, with the correct monochromator polarizer orientations know for the $6\,^3P$ forbidden lines, the light source polarizer was removed and the relative intensities of the NO($A\,^2\Sigma^+$, $v' = 0 \rightarrow X\,^2\Pi$, $v' = 0, 3, 4$) were observed ($\Delta\lambda = 40$ Å). Comparison of these intensities with the theoretical emission intensities of Zare *et al.*,[20] which have been shown to be in excellent agreement with experiment ($< \pm 10\%$),[19,21] yielded accurate relative detection efficiencies. The instrumental efficiency for 2656-Å line was linearly extrapolated from the $0 \rightarrow 3, 4$ band efficiency factors.

Third, the forbidden-line emission intensities were accumulated. The signal-plus-background and background counts were accumulated in eight, one-hour runs for each forbidden line, when the electron energy was adjusted to the $^3P_2$ excitation function peak ($E \simeq 5.75$ eV).

The result appropriate to Eq. (4) is

$$\frac{I_2(2270\ \text{Å})}{I_0(2656\ \text{Å})} = 7.56 \pm 0.60 . \qquad (6)$$

This result could be renormalized to other NO($A \rightarrow X$) emission intensities readily.[22] Using the transition probabilities of Garstang,[9] we conclude that

$$\frac{\sigma_2}{\sigma_0}\ (E \simeq 5.75\ \text{eV}) = 9.11 \pm 0.73 . \qquad (7)$$

The error in the cross-section ratio (7) reflects only the statistical uncertainties (± 2 standard deviations) in the detection efficiency factor and forbidden-line intensity-ratio measurements.

V. DISCUSSION

A. Hg($6\,^3P_2$)

The most recent $6\,^3P_2$ excitation functions are compared in Fig. 3. It is apparent that the results of Borst compare most favorably with this work, even to the extent of a small structure located in the vicinity of 7.5 eV. Although there is significant discrepancy in the threshold region, the difference can be attributed to our broader electron-energy spread.

It is possible that the structure at 7.5 eV is a contribution to the $6\,^3P_2$ state from an excited autoionizing state of $(\mathrm{Hg}^-)^*$. The neutral state that lies closest to this energy is the $7\,^3S_1$ (7.73 eV) which eliminates a cascade contribution. A small resonant-like structure around 7.5 eV has been seen in the electron transmission experiments of Burrow.[23] Evidence to support the general notion of autoionization here comes from the work of Fano and Cooper[24] and Hg($6\,^3P_1$) resonant structure studies of Zapesochnyi and Shpenik[25] and Ottley and Kleinpoppen.[26]

The interpretation above assumes that the electron-energy calibration of Borst (and therefore

ours) is correct, i.e., linear extrapolation of the $6\,^3P_2$ excitation function to $^3P_2$ threshold energy (5.46 ± 0.1 eV). This procedure could be incorrect, in part, if substantial contribution to the $6\,^3P_2$ state were coming from the $Hg^-(^2D_{5/2})$ resonance which has been classified by Heddle[27] to be the 5.50 eV resonance. The work of Burrow and Michejda[28] indicates a broad resonance at approximately that energy which might have been indistinguishable from the nonresonant contribution to $6\,^3P_2$ even at the energy resolution of Borst. If Borst's energy scale were recalibrated to allow for this possibility and if his error limits for linear extrapolation are considered (± 0.1 eV), then the structure around 7.5 eV (Fig. 3) would almost correspond to the energy of $7\,^3S_1$. The interpretation that eliminated the possibility of a $7\,^3S_1 \rightarrow 6\,^3P$ cascade would then not be strong.

The excitation function of Korotkov and Prilezhaeva deduced from their superelastic scattering measurements is about a factor of 2 (FWHM) more narrow than the measurements previously discussed. Also, no evidence of a weak structure near 7.5 eV is visible in their data.

Recent calculations of the $Hg(6\,^3P_2)$ excitation function have been reported[29,30] and compared to measurements.[2,3,29] Since the calculation of Moiseiwitsch and McConnell[30] has not been compared to experiment previously, it is shown in Fig. 3. In general agreement with other theoretical work noted, the calculation of Moiseiwitsch and McConnell disagrees with all measurements near threshold but parallels the measurements beyond about 6.5 eV. This lack of agreement might be attributable to a substantial broad resonant contribution to $Hg(6\,^3P_2)$ near threshold, as discussed above.

B. $Hg(6\,^3P_0)$

Experimental and theoretical excitation functions for $6\,^3P_0$ are compared in Fig. 4. The principal discrepancy in the measurements is width. Our excitation function is about a factor of 2 (FWHM) broader than that of Korotkov, and this discrepancy was also noted in the $Hg(6\,^3P_2)$ comparison. The superelastic scattering technique does not appear to yield detailed features of $Hg(6\,^3P_{0,2})$ excitation functions with great fidelity, but there is consistency in its shortcoming.

Detailed features in the measurements are also in disagreement. Korotkov found two distinct peaks in the excitation function ($E \simeq 4.8$, 5.15 eV). We observed two barely resolvable structures ($E \simeq 4.8$, 5.2 eV) in the near-threshold region. The electron-energy spread in both studies was comparable.

Originally, we believed our measurement to be structureless. But the 4.8-eV peak was repeated in more than 80% of the trials. Additional data at higher current density (greater electron-energy spread) revealed only a shoulder in the vicinity of 4.8 eV. Assuming our 4.8-eV structure is not an artifact and that the electron-energy calibration is essentially correct, then it is likely that the low-lying structure found by Korotkov has been verified. As suggested by Heddle,[27] this peak could be the $Hg^-(^4P_{3/2})$ resonant contribution (4.68 eV) to $Hg(6\,^3P_0)$. However, if our electron energy calibration were erroneously low as discussed in Sec. V A, then our 4.8-eV structure in Fig. 4 closely matches the location of the $Hg^-(^2D_{3/2})$ resonance located at 4.91.[27] It is also possible, parallel to the $Hg(6\,^3P_2)$ discussion, that the broad

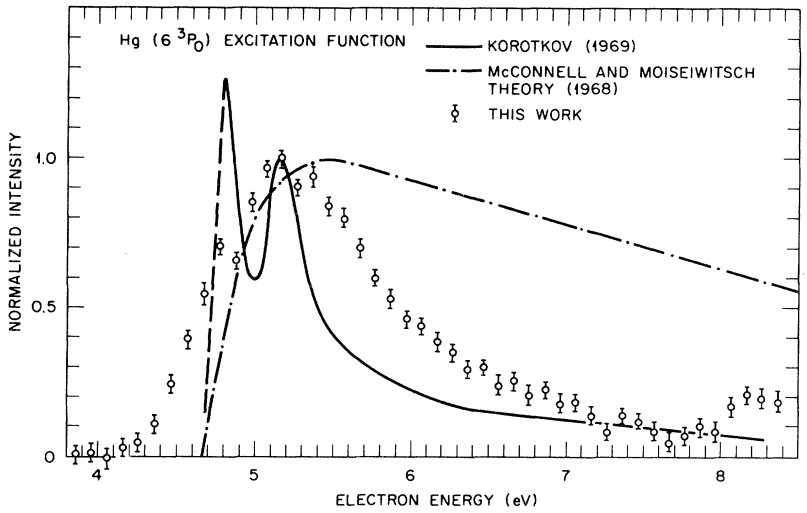

FIG. 4. Experimental and theoretical excitation functions for $Hg(6\,^3P_0)$. The experimental results in the vicinity of 5.2 eV have been normalized to the theoretical peak value. Data of Fig. 2 are shown.

$Hg^-(^2D_{5/2})$ resonance could have gone unresolved in the vicinity of 5.50 eV. Clearly, the $6\,^3P_0$ excitation function will have to be investigated in the near-threshold region at much higher electron-energy resolution if the uncertainties discussed above are to be resolved.

The weak structure in the $^3P_2$ excitation function at 7.5 eV is certainly not obvious in the $^3P_0$ excitation function; however, the data here are of poorer quality. The peak in the vicinity of 8.3 eV could be cascade or resonant contributions. Studies of Hg($6\,^3P_1$) excitation[26] also reveal structure in this vicinity.

Our $^3P_{2,0}$ measurements could not be extended to higher energies because very intense optical emission was observed beyond 8.5 eV. The origin of this light was probably radiative decay ($2500 < \lambda < 2800$ Å) of numerous excited states of Hg resulting from the intermultiplet quenching of high-lying metastable states of Hg (by collision with residual gas), such as the well-known Hg($5d^9 6s^2 6p, {}^3D_3$) state (8.785 eV).[1]

C. Cross-section ratio, σ_2/σ_0

The ratio of cross sections for the $^3P_{2,0}$ states has been measured at an electron energy corresponding to the peak of the $^3P_2$ excitation function ($E \simeq 5.8$ eV). The accuracy of the ratio result [Eq. (7)] is probably limited by the accuracy of Garstang's forbidden-line transition probabilities (i.e., A_2/A_0) since the error introduced by assuming theoretical emission intensities of NO($A \to X$) in the relative detection efficiency measurements must be small.[21] Also, the magnetic field (~5 G) in our observation zone probably affected the atomic transition probabilities in only a minor way.[12]

The matrix elements of the forbidden-line transitions computed which included "relativistic corrections, should be reasonably reliable; the neglect of configuration interaction is their major source of uncertainty."[9] Accuracy of the ratio, A_2/A_0 is probably better than the accuracy of A_2 or A_0 alone (±20%) because about half of the uncertainty in the A_i reflects the experimental uncertainty in $A_1(6\,^3P_1 \to 6\,^1S_0)$ to which A_2 and A_0 are normalized.[31] Note also that the calculation of A_0 by Bigeon[32] agrees with that of Garstang within 6%. Pessimistic accuracy limits attained by the measurements and calculations are ±30%.

An updated cross-section ratio [Eq. (7)] could be derived by the use of higher-accuracy forbidden-line transition probabilities with the Eq. (6) result via Eq. (4).

Of interest is the ratio of cross sections $(\sigma_2/\sigma_0)^P$ at the peak of each excitation frunction [$^3P_2$, $E \simeq 5.8$; $^3P_0$, $E \simeq 5.2$ (see Figs. 3 and 4)]. Based on our $^3P_0$ excitation function the result of this work is $(\sigma_2/\sigma_0)^P \cong 5.2$. Assuming the most extreme accuracy limits discussed above, this result is not in disagreement with the peak cross section ratio of Korotkov, ≈ 6.7 ($\sigma_2^P \cong 2.8 \times 10^{-16}$ cm^2, $\sigma_0^P \cong 0.42 \times 10^{-16}$ cm^2).

When our direct ratio result at the peak of the $6\,^3P_2$ states ($\sigma_2/\sigma_0 = 9.11$) is compared to that of Korotkov, $\sigma_2/\sigma_0 \cong 22$ ($E \cong 5.8$ eV, $\sigma_2 \cong 2.8 \times 10^{-16}$ cm^2, $\sigma_0 \cong 0.13 \times 10^{-16}$ cm^2), then the results are certainly in disagreement. We noted previously (Sec. V B) difficulty of measuring excitation functions via their superelastic scattering technique, and the above result reaffirms the statement since the above comparison depends only on the excitation function of Korotkov and not our own (equivalent electron-energy spread). Evidently, the technique of Korotkov applied to Hg($6\,^3P_{0,2}$) produced credible peak absolute cross sections (neglecting the 4.8-eV structure) but again not detailed shapes of the excitation functions. The peak absolute cross sections of Korotkov and Borst for $6\,^3P_2$ are in good agreement.

Our peak cross section ratio, $(\sigma_2/\sigma_0)^P = 5.2$, can be compared to the theoretical work. For Savchenko[29] and McConnell and Moiseiwitsch,[30] these results are about 3.2 and 3.5, respectively. Theoretical and experimental disagreement of the ratios is not surprising considering the excitation function discrepancies near threshold previously noted. Aside from possible effects resulting from neglect of resonant contributions to the $6\,^3P_{0,2}$ states in the calculations, the theoretical and experimental disagreements are not understood.

ACKNOWLEDGMENT

The authors are indebted to P. D. Burrow for helpful discussions at the conclusion of these experiments and for making his data available to us prior to publication.

*Research sponsored by the U. S. Energy Research and Development Administration under contract with Union Carbide Corporation.

†Present address: GTE Sylvania, Danvers, Mass.

[1] H. F. Krause, S. G. Johnson, S. Datz, and F. K. Schmidt-Bleek, Chem. Phys. Lett. 31, 577 (1975).
[2] W. L. Borst, Phys. Rev. 181, 257 (1969).
[3] A. I. Korotkov and N. A. Prilezhaeva, Sov. Phys. J. 13,

1625 (1970).
[4]A. I. Korotkov, Opt. Spektrosk. 28, 641 (1970) [Opt. Spectrosc. 28, 347 (1970)].
[5]S. G. Johnson, thesis, University of Tennessee, 1974 (unpublished).
[6]C. B. Moore, *Atomic Energy Levels*, NBS Circ. 467 (U.S. GPO, Washington, D. C., 1958), Vol. 3, pp. 192–195.
[7]S. Mrozowski, Z. Phys. 108, 204 (1938).
[8]S. Mrozowski, Phys. Rev. 67, 161 (1945).
[9]R. H. Garstang, J. Opt. Soc. Am. 52, 845 (1962).
[10]R. H. Garstang, Astrophys. J. 148, 579 (1967).
[11]M. Baumann, Z. Phys. 173, 519 (1963).
[12]P. P. Feofilov, *The Physical Basis of Polarized Emission* (Consultants Bureau, New York, 1961), pp. 54–87.
[13]J. M. Woolsey and J. W. McConkey, J. Opt. Soc. Am. 58, 1309 (1968).
[14]H. F. Krause, S. Datz, and S. G. Johnson, J. Chem. Phys. 58, 367 (1973).
[15]H. S. W. Massey, E. H. S. Burhop, and H. B. Gilbody, *Electronic and Ion Impact Phenomena* (Oxford U. P., London, 1971), Vol. 3, p. 1693.
[16]F. J. van Itallie, L. J. Doemeny, and R. M. Martin, J. Chem. Phys. 56, 3689 (1972).
[17]R. Burnham and N. Djeu, J. Chem. Phys. 61, 5158 (1974).
[18]D. A. Hutchison and J. R. Wolff, Rev. Sci. Instrum. 25, 1083 (1954).
[19]H. F. Krause and S. Datz, Chem. Phys. Lett. 41, 339 (1976).
[20]D. L. Albritton, A. L. Schmeltekopf, and R. N. Zare, Computer Routine for Calculating Diatomic Intensity Factors, RKR version 1.4, FCF version 1.2, 1972 (unpublished).
[21]H. M. Poland and H. P. Broida, J. Quant. Spectrosc. Radiat. Transfer 11, 1863 (1971).
[22]To renormalize the result to a different set of $NO(A^2\Sigma^+, v'=0 \rightarrow X\,^2\Pi, v''=0,3,4)$ emission intensities of the form $I_{0,0}:I_{0,3}:I_{0,4}=1.00:I_{0,3}:I_{0,4}$, multiply Eq. (6) and (7) values by the factor $(0.2344/I_{0,3}+0.1596/I_{0,4})$. The relative intensities for photoelectric detection used were 1.00:0.570:0.271. These include relative R^2_{centroid} factors.
[23]P. D. Burrow (private communication).
[24]U. Fano and J. W. Cooper, Phys. Rev. 138, A400 (1965).
[25]I. P. Zapesochnyi and D. B. Shpenik, Zh. Eksp. Teor. Fiz. 50, 890 (1966) [Sov. Phys.–JETP 23, 592 (1966)].
[26]T. W. Ottley and H. Kleinpoppen, J. Phys. B 8, 621 (1975).
[27]D. W. O. Heddle, J. Phys. B 8, L33 (1975).
[28]P. D. Burrow and J. A. Michejda, in *Electron and Photon Interactions with Atoms*, edited by H. Kleinpoppen and M. R. C. McDowell (Plenum, New York, 1975).
[29]V. I. Savshenko, Opt. Spektrosk. 30, 12 (1971). [Opt. Spectrosc. 30, 6 (1971)].
[30]J. McConnell and B. Moiseiwitsch, J. Phys. B 1, 406 (1968).
[31]R. H. Garstang (private communication).
[32]M. C. Bigeon, J. Phys. (Paris) 28, 51 (1967).